STUDY OF AN INCLINED INTERFACE OF CONTACT USING LATTICE BOLTZMANN METHOD

by

Oussama El MHAMDI and Elalami SEMMA

Laboratory of Engineering Industrial Management and Innovation,
University Hassan 1[st], FST Settat, Morocco

Original scientific paper
https://doi.org/10.2298/TSCI170712212E

The lattice Boltzmann method and the particle image model are adopted to study a heat transfer problem with thermal contact resistance. In this paper, a new study involving an inclined interface of contact between two media is introduced in order to evaluate a 2-D heat transfer in the steady regime. A case of study and numerical results are provided to support this configuration. The obtained results show the effect of the thermal contact resistance on the heat transfer, as well as the temperature distribution on the two contacting media.

Key words: *lattice Boltzmann method, thermal contact resistance, particle image model, inclined interface of contact*

Introduction

The lattice Boltzmann method (LBM) is a successful numerical modeling method based on the simulation of collision and streaming processes across a limited number of particles, which has an excellent stability and an important role in simulations of micro and macro fluid-flows. Compared to the traditional CFD methods, LBM has many advantages especially in applications involving complex geometries and porous media. This method has proved its effectiveness in the field of conventional fluid-flow and it has been used in many applications in simulating isothermal flows in the last years [1-3]. In addition, there have been studies aiming to construct a stable thermal lattice Boltzmann method (TLBM) to solve heat transfer problems. He *et al*. [4] introduced a model based on a double population approach and which has a good numerical stability. This model has been used by researchers to solve different thermo-hydrodynamic problems [5-7].

In heat transfer problems and more precisely, in modeling thermal contact resistance (TCR), on the one hand, Han *et al*. [8]. introduced a novel numerical approach, the partial bounce back scheme (PBB), to account for TCR between contacting surfaces within the framework of the thermal LBM, and Xie *et al*., [9] studied thermal conduction in composites with TCR. On the other hand, El Ganaoui *et al*. [10] introduced the particle image (PI) model which is a numerical approach for the thermal LBM to solve problems with contact resistance between surfaces and El Mhamdi and Semma [11] established an overall comparison between these two models in order to determine the most accurate one.

The TCR exists due to many reasons such as surface irregularities and impurities which represent a barrier to the normal circulation of heat flux. This phenomenon causes an interfacial

Corresponding author, e-mail: oussama.elmhamdi@gmail.com

gap between two contacting surfaces and has important impact in many applications like electronic packaging and composite materials design and manufacture. This practical application explains the interest of these studies.

Thermal lattice Boltzmann method for 2-D model

As previously said, the LBM consists of two steps, collision and streaming. These two steps are described by the following equations:

Collision:

$$f_i(x, y, t+\Delta t) = f_i(x, y, t) - [f_i(x, y, t)] - f_i^{eq}(x, y, t)] \text{ for } 0 \le i \le n \tag{1}$$

Streaming:

$$f_i(x+\Delta x, y+\Delta y, t+\Delta t) = f_i(x, y, t+\Delta t) \text{ for } 0 \le I \le n \tag{2}$$

When n is the number of neighboring nodes.

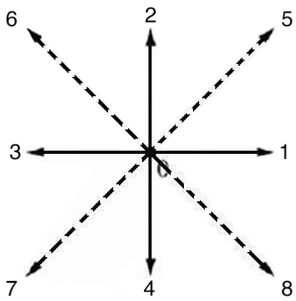

Figure 1. The nine possible vectors of movement for D2Q9 model

In the most used D2Q9 model, the particles at each node can remain at their positions or move to their eight adjacent nodes as shown in fig. 1. The nine discrete velocities of these movements e_i are given in eq. (3). And to each one corresponds a weighting coefficient w_i as given in eq. (4).

$$e_i = \begin{cases} 0 \text{ for } i = 0 \\ c\,(\pm 1, 0) \text{ and } c\,(0, \pm 1) \text{ for } 1 \le i \le 4 \\ c\,(\pm 1, \pm 1) \text{ for } 5 \le i \le 8 \end{cases} \tag{3}$$

where c is the lattice speed, which is given by $c = \Delta x / \Delta t$ with Δx being the lattice spacing and Δt the time step.

$$w_i = \begin{cases} 4/9\ 0 \text{ for } i = 0 \\ 1/9 \text{ for } 1 \le i \le 4 \\ 1/36 \text{ for } 5 \le i \le 8 \end{cases} \tag{4}$$

The D2Q9 model allows to write:

Temperature

$$T(x, y, t) = \sum f_i(x, y, t) \text{ for } 0 \le i \le 8 \tag{5}$$

Flux

$$q = \sum e_i f_i(x, y, t) \text{ for } 0 \le i \le 8 \tag{6}$$

where T and q are, respectively, the temperature and the heat flux at each node.

More precisely, in modeling TCR, two models have been introduced: the partial bounce back (PBB) model and the PI model. In the following chapter, an overall comparison between these two models is provided in order to determine which one is the most accurate.

Numerical models

The partial bounce back model [8]

The PBB model is introduced to solve problems with TCR between two bodies. It assumes that only a proportion of the thermal energy of the first body can be transmitted to the second, when the remaining energy rebounds towards the first body itself in the opposite direction as shown in fig. 2.The rebounded proportion is represented by the parameter, δ, (PBB parameter) which is included between 0 and 1.

In this model, the TCR is given by:

$$Rc = \frac{3\delta}{1-\delta} \tag{7}$$

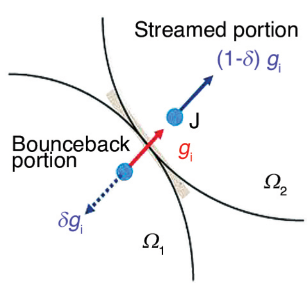

Figure 2. The PBB scheme [8]

In fact, for a given density function g_i, the proportion (1-δ) g_i is transmitted from the node I, which belongs to the body 1, to the adjacent node J which belongs to the body 2. The remaining proportion δg_i rebounds to the node I itself.

The particle image model [10]

This model assumes that both borders in contact are juxtaposed and their distribution functions during the propagation are proportional. For the distribution functions represented in fig. 3, and in the isotropic case, the proportionality is expressed by two matrix relationships:

$$\begin{pmatrix} f_3 \\ f_6 \\ f_7 \end{pmatrix} = \alpha I_\mathrm{d} \begin{pmatrix} g_3 \\ g_6 \\ g_7 \end{pmatrix} \text{ and } \begin{pmatrix} g_1 \\ g_5 \\ g_8 \end{pmatrix} = \beta I_\mathrm{d} \begin{pmatrix} f_1 \\ f_5 \\ f_8 \end{pmatrix} \quad (8)$$

With I_d is the 3×3 identity matrix, f_i, density functions related to the medium 1 for $0 \leq I \leq 8$, g_i, density functions related to the medium 2 for $0 \leq i \leq 8$. In order to evaluate the parameters α and β, we use the following equations:

$$q_{12} = q_{21} \quad (9)$$

$$q_{12} = \frac{\Delta T}{Rc} \quad (10)$$

where q_{12} is the heat flux transmitted from medium 1 to medium 2, q_{21}, – heat flux transmitted from medium 2 to medium 1, ΔT – the temperature jump at the contact interface.

Comparisons

The comparisons cover both transient and steady regimes and concern the case represented in fig. 3, where the contacting media are equally sized rectangular bars with TCR at the interface. The bars have the same initial temperature $T_i = 0$. During the simulation, the left and right walls are maintained at different constant temperatures with $T_\mathrm{left} = 0$ and $T_\mathrm{right} = 1$, when the top and bottom walls are adiabatic to ensure a one-dimensional heat conduction situation.

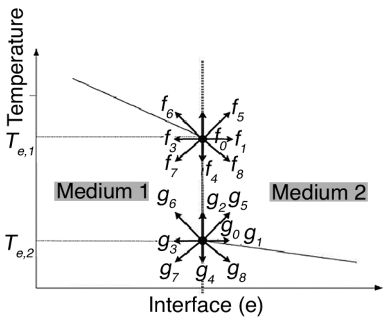

Figure 3. Configuration diagram for the PI model LBM [10]

Transient regime

El Ganaoui *et al* [10] made a comparative study between the two models while validating the PI model and its accuracy. The comparison covered a large range of relaxation time from 0.55 to 1. For τ =1, the two models exhibit accurate agreement with the analytical solution, as shown in fig. 4. This value of relaxation time (τ = 1) corresponds to the hypothesis of the permanent regime introduced by Han *et al*, [8]:

$$f_2 = f_4 = f_2^\mathrm{eq} = \frac{1}{6} T \quad (11)$$

Figure 5 gives the temperature profile at t = 5000, for τ = 0.8 and Rc = 1000. The PBB model exhibits a difference with the analytical solution. This inaccuracy can be explained by the underestimate of the functions f_2 and f_4 in the steady regime. For weak values of the relaxation time, the PI model reaches the analytical solution, when the PBB model show more deviation as show in fig. 6 and 7.

This study shows that the PBB gives accurate results when τ = 1, and exhibits inaccuracy when $0.55 \leq \tau < 1$. In fact, the further the relaxation time is from the value 1, the more inaccurate goes the PBB model, when the PI model still reaches the analytical solution even for low values of relaxation time.

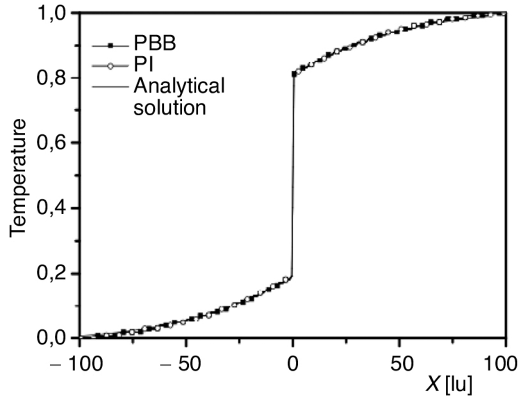

Figure 4. Temperature distribution (τ = 1, t = 10000, Rc = 1000) [10]

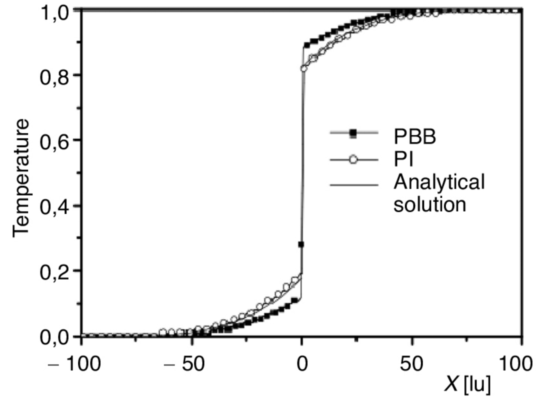

Figure 5. Temperature distribution (τ = 0.8, t = 5000, Rc = 1000) [10]

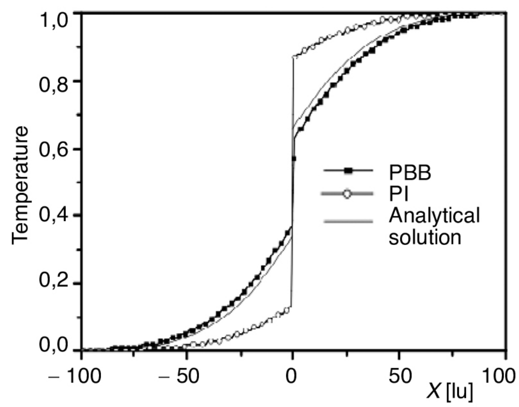

Figure 6. Temperature distribution (τ = 0.6, t = 20000, Rc = 1000) [10]

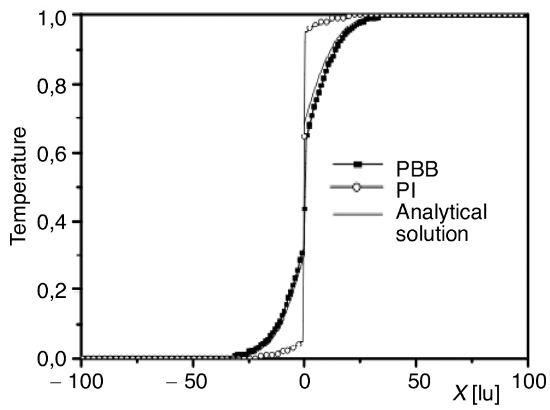

Figure 7. Temperature distribution (τ = 0.55, t = 5000, Rc = 1000) [10]

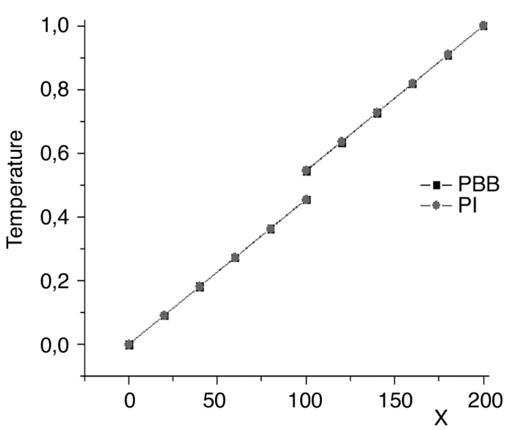

Figure 8. Temperature distribution in space Rc = 20 [11]

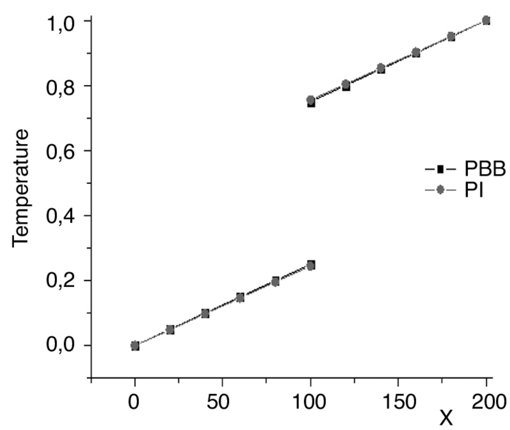

Figure 9. Temperature distribution in space Rc = 200 [11]

Steady regime

El Mhamdi and Semma [11] achieved a comparison between the two models in the steady regime. This comparison covered different values of the TCR as shown in figs. 8-11.

To sum up this overall comparison, the cases of study discussed have shown that the two models exhibit accurate agreement with the theoretical solution in the steady regime, when the PI model exhibits more accuracy in the transient regime. It can be deduced that the PI model is the most raccurate model for solving heat transfer problems with TCR. This is why we will be using the PI model in the study of the inclined contact interface.

Study of inclined contact interface

Initial state and boundary conditions

The study area is rectangular 80 × 40 representing two contacting media following a slope $s = 2$ as shown in fig. 12. Initially $(t = 0)$, the temperature of the medium 1 equals 0 and the temperature of the medium 2 equals 1. During the simulation, the left side of the medium 1 is maintained at $T_1 = 0$, while the right side of the medium 2 is maintained at $T_2 = 1$.With $\Delta x = \Delta y = \Delta t = 1$.

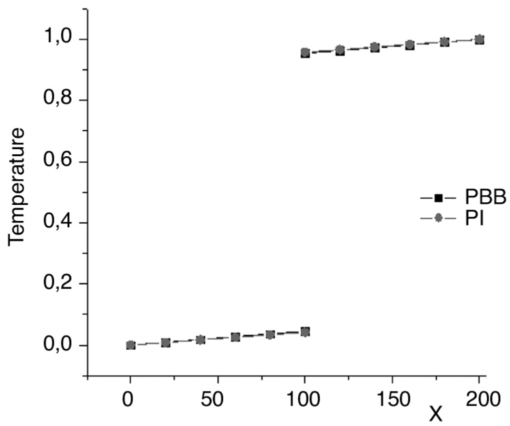

Figure 10. Temperature distribution in space *Rc* = 2000 [11]

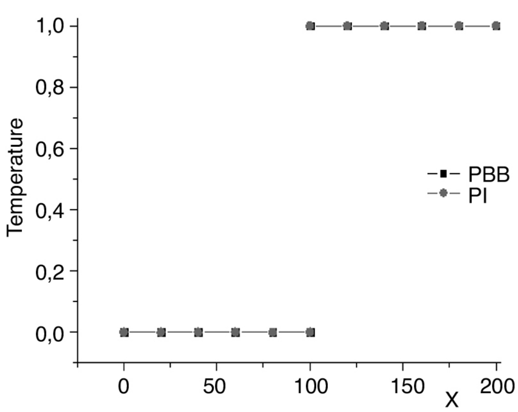

Figure 11. Temperature distribution in space *Rc* = ∞ [11]

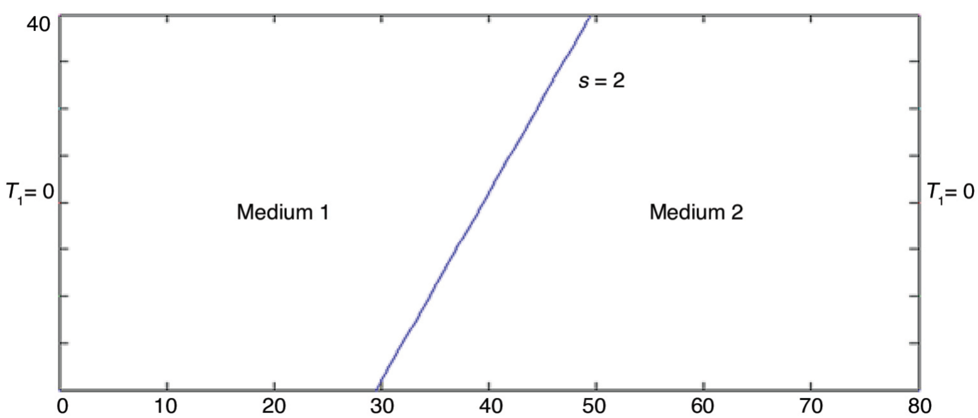

Figure 12. Configuration of inclined contact interface

Methodology of resolution

The main idea of solving this kind of problems consists in two steps: approaching the points on the contact interface with nodes on the lattice, and calculating the parameters of proportionality α and β at the interface of contact.

The first step is approaching the points on the contact interface with nodes on the lattice so we can use the LBM method. In fact, each point A with co-ordinates x_A and y_A belonging to the interface of contact can be approached by a node A' belonging to the lattice as shown in fig. 13. In order to achieve this approach, we can use the following mathematical algorithm, fig. 14:

$$x_A = \begin{cases} i \text{ if } x_A < i + 0.5 \\ i + 1 \text{ if } x_A >= i + 0.5 \end{cases} \quad y_A = \begin{cases} j \text{ if } y_A < j + 0.5 \\ j + 1 \text{ if } y_A >= j + 0 \end{cases}$$

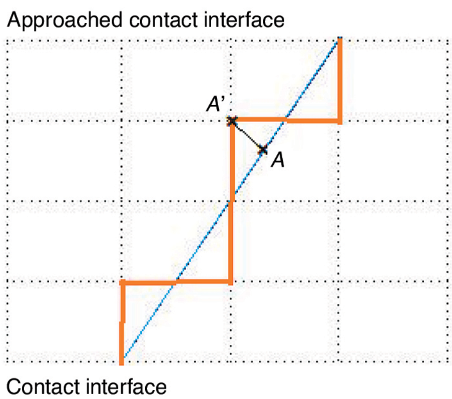

Figure 13. Lattice approach of the contact interface

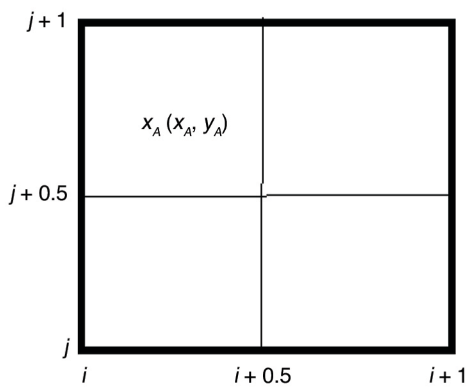

Figure 14. Node approach configuration

Study of nodes

After applying the algorithm all along the contact interface, we find an approached interface as shown in fig. 15. Then, we have to calculate the parameters of proportionality α and β for each node.

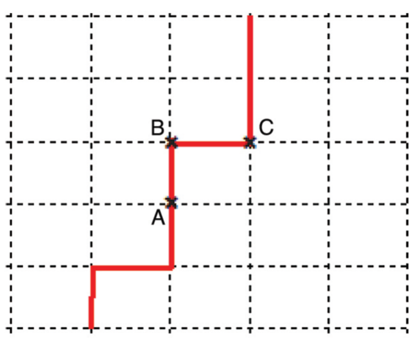

Figure 15. Approached contact interface

There are three cases, and to each case corresponds different parameters α and β as detailed hereafter.

For the node A and similar nodes on the approached contact interface, we have the same case as the configuration represented in fig. 3, where the unknown distribution functions are f_3, f_6, f_7, g_1, g_5, and g_8. The proportionality between the distribution functions is expressed in eq. (8).

For the node B and similar nodes, the unknown distribution functions are f_6, g_1, g_4, g_5, g_7, and g_8. The assumption of proportionality is expressed by the following relationships:

$$f_6 = \alpha_1 g_6 \text{ and } \begin{pmatrix} g_1 \\ g_4 \\ g_5 \\ g_7 \\ g_8 \end{pmatrix} = \beta_1 I_d \begin{pmatrix} f_1 \\ f_4 \\ f_5 \\ f_7 \\ f_8 \end{pmatrix} \tag{12}$$

Finally, for the node C and similar nodes, the uknown distributon functions are f_2, f_3, f_5, f_6, f_7, and g_8. The assumption of proportionality is expressed by the following relationships:

$$\begin{pmatrix} f_2 \\ f_3 \\ f_5 \\ f_6 \\ f_7 \end{pmatrix} = \alpha_1 I_d \begin{pmatrix} g_2 \\ g_3 \\ g_5 \\ g_6 \\ g_7 \end{pmatrix} \text{ and } g_8 = \beta_2 g_6 \tag{13}$$

With I_d is the 5 × 5 identity matrix.

In order to evaluate the parameters of proportionality α_1, β_1, α_2, and β_2 we can use eqs.(9) and (10).

Results and discussion

X-direction flux

In this part, we will have a view over the flow in the *X*-direction. Figures 16 and 17 represent, respectively, the temperature distribution for *Rc* values of 50 and 200, for different values of *y* (0, 20, and 40). Figures 15 and 16 show that the temperature gap at the contact interface is stable for different values of *y*. The length difference is due to the inclined interface between the contacting media.

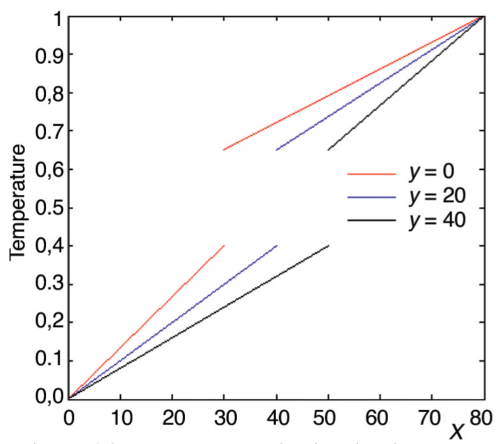

Figure 16. Temperature distribution in *X*-direction *Rc* = 50

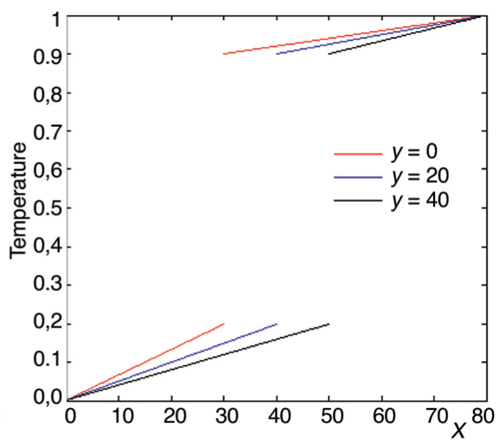

Figure 17. Temperature distribution in *X*-direction *Rc* = 200

The Y-directon flux

In this part, we will have a view over the flow in the *Y*-direction. figs.18 and 19 represent, respectively, the temperature distribution for *Rc* values of 50 and 200, for different values of *x* (10, 35, 45, and 70).

For both *Rc* values of 50 and 200, the temperature curve is continuous for $x = 10$ and $x = 70$ because these areas belong to the same medium ($x = 10$ belongs to the medium 1 and $x = 70$ belongs to the medium 2), while we can notice a discontinuity at $x = 35$ and $x = 45$ because of the conntact interface.

Influence of the thermal contact resistance

In this part, we will evaluate the influence of the TCR on heat transfer. Figure 20 represents the temperature distribution in *X*-direction at $y = 20$ for different values of *Rc* (50, 200, and 500) while fig. 21 represents the temperature distribution in *Y* - direction at $x = 20$ for the same values of *Rc*.

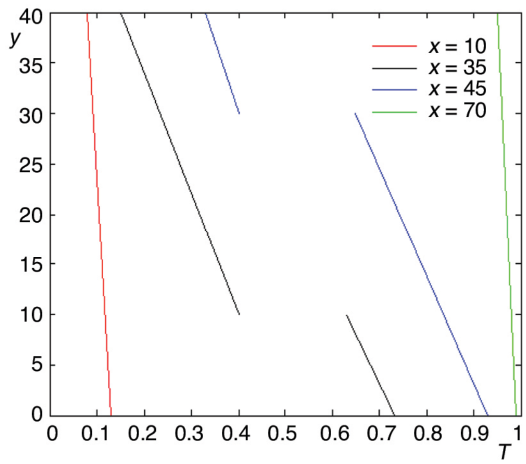

Figure 18. Temperature distribution in *Y*-direction *Rc* = 50

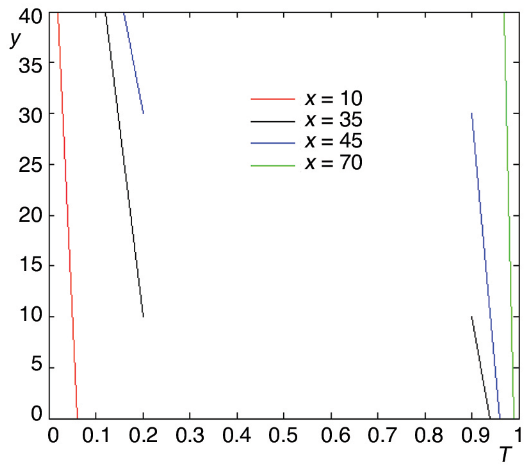

Figure 19. Temperature distribution in *Y*-direction *Rc* = 200

For low values of *Rc*, the temperature gap is small, and it gets bigger as *Rc* increases. When *Rc* equals ∞, there is no heat flow between the two media. These results can be justified by the effect of TCR, which prevents the perfect heat transfer. The simulated numerical values as well as the theoretical values of the temperature gap at the contact interface are illustrated in tab. 1, figs. 22 and 23 represent an overview on the thermal field for *Rc* = 50 and *Rc* = 200.

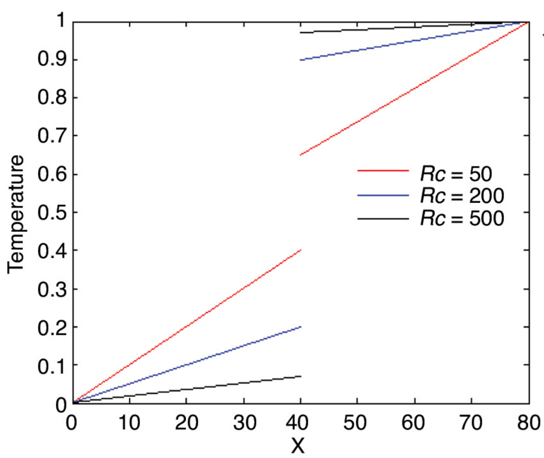

Figure 20. Effect of *Rc* (*y* = 20)

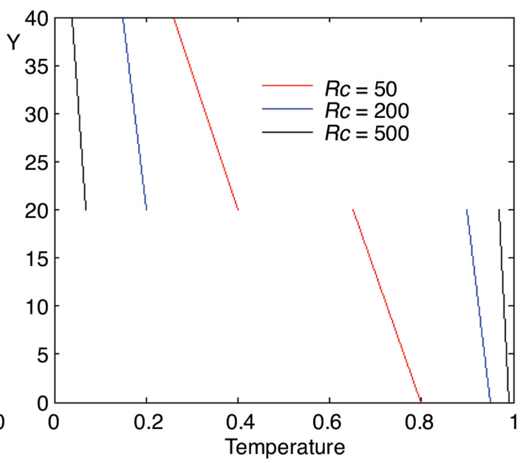

Figure 21. Effect of *Rc* (*x* = 20)

Table 1. Simulated and theoretical temperature gap at the contact interface

Rc	0	50	200	500	2000	∞
Theoretical gap	0	0.26	0.714	0.884	0.962	1
Simulated gap	0	0.253	0.703	0.902	0.978	1

Conclusion

In this paper, we presented an overall comparison between the PBB model and PI model and we established a new study of an inclined contact interface using lattice Boltzmann method in order to evaluate a 2-D heat transfer. The conclusions are the following:

- The PI model is accurate for both transient and steady regime, when the PBB model shows inaccuracy in the transient regime. So, the PI model is the most accurate.
- The simulated results show a temperature variation in *X*- and *Y*-directions so the 2-D heat transfer is ensured due to the flux at the inclined interface of contact.
- The simulated results show that the temperature gap at the contact interface is proportional to the thermal contact resistance. (The temperature gap increases when *Rc* increases and *vice versa*).

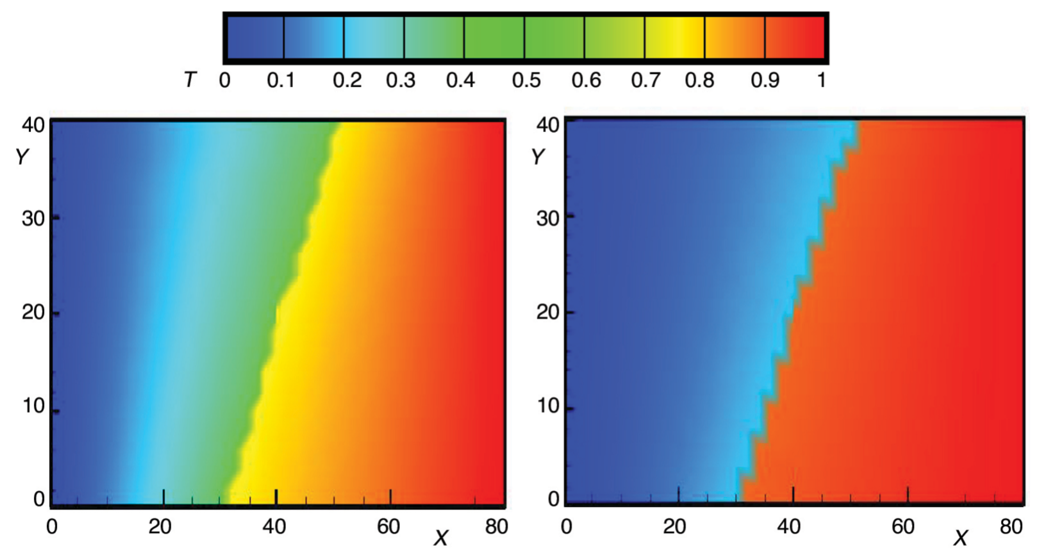

Figure 22. Thermal field, *Rc* = 50

Figure 23. Thermal field, *Rc* = 200

Nomenclature

t	– time, [s]
q	– heat flux, [J/sm^{-2}K]
T	– temperature [K]
Rc	– thermal contact resistance [−]

Greek symbols

Δx	– lattice spacing in x-direction, [m]
Δy	– lattice spacing in y-direction, [m]
Δt	– time step, [s]
δ	– partial bounce back parameter, [−]

References

[1] Guo, Z. L., *et al*., A coupled Lattice BGK Model for the Bouessinesq Equation, *Internat. J. Numer. Methods Fluids, 39* (2002), 4, pp. 325-342
[2] Wang, J. *et al*., A lattice Boltzmann Algorithm for Fluid Solid Conjugate Heat Transfer, *Int. J. Thermal Sci. 46* (2007), 3, pp. 228-234
[3] He, X., Luo, L.-S., Theory of the lattice Boltzmann method: From the Boltzmann Equation to the Lattice Boltzmann Equation, *Phys. Rev., E 56* (1997), G., pp. 6811-6817
[4] He, X., *et al*., A novel Thermal Model for the Lattice Boltzmann Method in Incompressible Limit, *J. Comput. Phys., 146* (1998), 1, pp. 282-300
[5] D'Orazio, A. Z., *et al*., Application to Natural Convection Enclosed Flows of a Lattice Boltzmann BGK Model Coupled with a General Purpose Thermal Boundary Condition, *Int. J. Thermal Sci., 43* (2004), G., pp. 575-586.
[6] Tang, G. H., *et al*., Thermal Boundary Condition for the Thermal Lattice Boltzmann Equation, *Phys. Rev., E 72* (2005), 1, pp. 016703
[7] Huang, H., *et al*., Thermal Curved Boundary Treatment for the Thermal Lattice Boltzmann Equation, *Int. J. Modern Phys., C 17* (2006), 5, pp. 631-643

[8] Han, K., *et al*., Modelling of Thermal Contact Resistance Within the Framework of the Thermal Lattice Boltzmann Method, *Int. J. Thermal Sci., 47* (2008), 10, pp. 1276-1283

[9] Xie, C., *et al*., Lattice Boltzmann Modeling of Thermal Conduction in Composites with Thermal Contact Resistance. *Communications in Computational Physics, 17* (2015), 4, pp. 1037-1055

[10] El Ganaoui, M., *et al.*, Analytical and Innovative Solutions for Heat Transfer Problems Involving Phase Change and Interfaces on the Aptitude of the Lattice Boltzmann Approach for the Treatment of the Transient Heat Transfer with Crack Resistance, *C. R. Mecanique 340* (2012),7, pp. 518-525

[11] El Mhamdi, O., Semma, E., Solving Heat Transfer Problems with Thermal Contact Resistance Using the Lattice Boltzmann Method*, Proceedings*, IEEE 4th International Conference on Wireless Technologies, Embedded and Intelligent Systems-WITS-2017, Fez, Morocco, 2017

Paper submitted: August 12, 2017
Paper revised: September 14, 2017
Paper accepted: September 19, 2017